Elucidating the structural features of ABCA1 in its heterogeneous membrane environment.

Sunidhi S.[a,1], Sukriti Sacher[a,1], Parth Garg[a], Arjun Ray[a,*]

[a] *Department of Computational Biology, Indraprastha Institute of Information Technology, Delhi, India*

Abstract

ABCA1 plays an integral part in Reverse Cholesterol Transport (RCT) and is critical for maintaining lipid homeostasis. One theory of lipid efflux by the transporter (alternating access) proposes that ABCA1 harbours two different conformations that provide alternate access for lipid binding and release, leading to sequestration via a direct interaction between ABCA1 and its partner, ApoA1. The alternative theory (lateral access) proposes that ABCA1 obtains lipids laterally from the membrane to form a temporary extracellular 'reservoir' containing an isolated pressurized lipid monolayer caused by the net accumulation of lipids in the exofacial leaflet. Recently, a full-length Cryo-EM structure of this 2,261-residue transmembrane protein showed its discreetly folded domains and conformations, as well as detected the presence of a tunnel enclosed within ECDs. While the tunnel was wide-enough at the proximal end for accommodating passage of lipids, the distal end displayed substantial narrowing, making it inaccessible for ApoA1. Therefore, this structure was hypothesized to substantiate the lateral access theory, whereby ApoA1 obtained lipids from the proximal end. Utilizing long time-scale multiple replica atomistic molecular dynamics simulations (MDS), we simulated the structure in a heterogeneous lipid environment and found that along with several large conformational changes, the protein widens enough at the distal end of its ECD tunnel to now enable lipid accommodation. In this study we have characterized ABCA1 and the lipid dynamics along with the protein-lipid interactions in the heterogeneous environment, providing novel insights into understanding ABCA1 conformation at an atomistic level.

Keywords: `ABCA1, Reverse Cholesterol Transport, MD Simulation`

*Corresponding author

Email address: `arjun@iiitd.ac.in` (Arjun Ray)

[1] Equal Contribution

Introduction

ATP Binding Cassette transporters constitute a ubiquitous superfamily of integral membrane proteins that couple transport of a chemically diverse set of substrates across bilayers to hydrolysis of ATP. The ABCA subfamily that includes ABCA1, is involved in transportation of lipids across the membrane[1]. ABCA1 plays a pivotal role in Reverse Cholesterol Transport (RCT) by facilitating the unidirectional net efflux of free cholesterol and phospholipids to poorly lipidated ApoA1 in plasma. This affiliation leads to formation of nascent HDL[2]. The physiological importance of ABCA1 is underscored by its association with various dyslipidaemic disorders such as familial HDL deficiency and Tangier disease, both of which are characterized by accumulation of cholesteryl esters in peripheral cells, particularly macrophages[3]. Moreover, ABCA1 mutant mice show diminished LCAT activity and a lack of alpha migrating HDL particles and pre-βHDL particles rich in triglycerides with altered phospholipid distribution, highlighting its role in nascent HDL formation[4, 5]. This is also supported by in vitro models that have concluded a consequent failure in nascent HDL generation on incubation of ApoA1 with cells lacking in ABCA1[2].

ABCA1 is a full transporter made up of 2,261 residues that form six domains: two transmembrane domains (TMDs) consisting of six membrane-spanning helices each); two nucleotide binding domains (NBDs) in the cytoplasm that serve to couple ATP hydrolysis to translocase activity; and two large extracellular domains (ECDs) that are implicated in protein-protein interactions as well as regulatory roles (Figure 1A). High resolution structures of NBDs of bacterial vitamin B12 importer, BtuCD as well as dimeric multidrug exporter, Sav1886 have aided in elucidation of mechanism of substrate translocation. The binding of two ATP molecules in the conserved Walker A and Walker B motif of NBDs leads to a conformational change such that the TMDs form an outward facing cavity that facilitates substrate binding. Hydrolysis of ATP puts an end to this cycle by separating the NBDs, driving TMDs to form an inward facing cavity that forms a passage for export of substrate[1]. The recent cryo EM crystal structure of ABCA1 however unveiled a snapshot of the protein such that these TMDs were found to face outwards, exposed by lipids on all sides. Additionally, it also revealed a polar cluster on one side of TMD1 that was speculated to bind polar groups of lipids and facilitate their flopping movement across the hydrophobic barrier. The structure also notably did not have a central cavity in the TMD region due to which the mechanism of "lateral access" for substrate entrance from the membrane inner leaflet was proposed. Moreover, the two extended ECDs were found to adopt a novel fold. ECD1 folded into 21 α helices and 10 β strands that made up 4 distinct regions: a base domain, helical domain 1 and 2 and a lid domain while ECD2 folded into 6 α helices and 7 β sheets[6]. The two ECDs packed tightly against each other with help of 4 disulfide bonds (Cys75-Cys309, Cys54-Cys81, Cys355-Cys504 in ECD1 and Cys1465-Cys1477 in ECD2), two of which have been shown to be necessary for ApoA1 binding and HDL formation[7]. They also enclose a tunnel $\sim$60 Å in height that is surrounded by hydrophobic residues that can serve as temporary storage or

delivery passage for lipids to the extracellular milieu[6, 8]. Moreover, ECDs have been reported to undergo conformational change in response to ATP hydrolysis resulting in ApoA1 binding, accentuating their role as temporary lipid reservoirs[9].

Although the role of ABCA1 in RCT has long been established, its functional characterization on the membrane requires more work. It is reported that ABCA1 translocase activity leads to lipids reorganization such that free cholesterol in the membrane is more accessible to cholesterol oxidase. This reorganization is believed to be due to the partitioning of ABCA1 into non-raft domains caused by destabilization of rafts[10, 11]. In addition to ApoA1 dependent export of excess cholesterol, ABCA1 is also involved in flopping cholesterol from inner to outer leaflet of the plasma membrane[12]. While several studies have biochemically characterized ABCA1 activity on the membrane and its involvement in nascent HDL generation, no work has been done to explicate ABCA1's interaction with adjacent membrane lipids at an atomistic resolution. In this study we have employed the use of all atom molecular dynamics to simulate ATP unbound ABCA1 monomer in an explicit heterogeneous membrane bilayer to refine the original model. We have elucidated the effect of ABCA1 on membrane dynamics as well quantitated the protein-protein as well as the protein-lipid interactions that impact its stability.

Deciphering the stable structural elements of the ABCA1 protein.. We were interested in elucidating the stable state of the ATP-unbound ABCA1 in a heterogeneous lipid bilayer. Using multiple long scale (1.0 μs each) all-atom classical molecular dynamics, we established the stable conformation of the protein in a heterogeneous lipid membrane. In order to understand the deviation of the protein from the Cryo-EM structure RMSD and Rg values of all the simulations were calculated for the backbone atoms of the protein. It was observed that the final structure from the simulated trajectory stabilized with $\sim$ 1.2 nm deviation from the initial structure. This stable structure showed an increase of 0.15 nm in its Rg value (Supplementary Figure 1). The energy landscape of all the conformations in each of the replicate simulations based on RMSD as well as Rg values revealed that the protein conformation initially clustered at 1.2 RMSD and 6.25 Rg (coloured dark blue in Figure 1B) while the final conformation lay in the range of 1.2-1.4 RMSD and 6.32-6.43 Rg (coloured sea green in Figure 1B). The final structure from the simulated trajectory showed a difference of 4Kcal/mol from the initial Cryo-EM structure. The analysis of the structural fluctuations throughout the simulation length revealed higher fluctuations ($>$ 1nm) in the extremities of the protein structure, notably in ECD1 and NBD1 and NBD2, while the major portion of the protein remained relatively stable throughout the simulation (Figure 1C & Supplementary Figure 2). This result is not unexpected since both regions are well exposed with water and are known to undergo conformational changes during the translocation cycle[9, 13]. Next, we utilized all the simulations to elucidate the secondary structure assignment of each residue. The probability of every residue to conform to a particular secondary structural element was calculated and a secondary struc-

ture was assigned to it based on its propensity to conform to this secondary structure for 70% of times throughout the simulation. We observed that the protein residues majorly favoured to exist as helix (39% residues) followed by coil (15% residues), while beta-sheet and turn were least favoured (4.5% and 1.5% respectively) (Figure 1D & Supplementary Figure 3). Additionally, it was observed that most of the helices that make up the protein were fairly rigid (blue, helix angle close to 0) while a few of them displayed a fair degree of bending (red) (Figure 1F). Surprisingly, 40% residues, i.e 921 residues, displayed fast dynamics for inter-change of secondary structures throughout the simulation. The percentage of these dynamical residues that make up each of the functional domains of the protein are shown in Figure 1E and they appear to be equally distributed throughout all the domains.

We also characterized the tunnel enclosed within the protein. A comparative volume as well as diameter profile of the crystal structure with respect to the average structure from the simulation has been shown (Figure 2A & Supplementary Figure 4). The volume profile depicts radical changes in the pore volume of the simulated structure compared to the crystal structure ($\sim$ 60,000 $\AA^3$). The simulated structure appears to be more extended while differences in diameter as well as volume of the tunnel enclosed within TMDs and ECDs show drastic variations between the two structures. A central cavity traverses the entire protein. At $\sim$ 95-100 Å the volume profile shows narrowing of the pore which coincides with TMD1 and TMD2 coming closer to each other. It then continues into the extracellular domain where its proximal opening is marked at the based of ECD1 at around 150 Å. This opening is wide enough in both the crystal as well as simulated structure. The volume of the distal opening of ECD tunnel (at $\sim$ 180 Å) in our simulated structure however is 4 times the volume reported for the crystal structure (Figure 2B). Qian et al. had proposed that the narrowing of the distal end suggests a probable mechanism where ApoA1 associates at the base of ECD1, to obtain lipids from the proximal end[6]. Our structure however shows that it may be possible to associate at the distal end of the tunnel as well. We also observed that the residues that line the tunnel especially the portion enclosed by ECDs and TMDs are majorly hydrophobic in character (Figure 2C). This isn't unexpected as these regions are implicated in lipid export. Additionally, we also found that most of the pathogenic residues[14, 15, 16, 17, 18, 19, 20, 21] that were found to line the inner cavity in both the crystal as well as simulated structure clustered at the cusps of ECDs as well as in the cystoslic region that constitutes NBD1 highlights the critical role of these functional domains (Supplementary figure 4). We also compared the two structures based on their contacts and the observed differences are summarized in their respective contact maps (Supplementary Figure 5). The contact map shows differences in contacts between res 750-1500 with res 1800-2216. These regions correspond to TMD1, ECD2 and NBD2 respectively. Additionally, we also analyzed the protein-protein interaction network of the crystal structure compared to our simulated structure (Supplementary Figure 6). Such a network representation has the ability to demonstrate the difference at the detailed residue interaction level by highlighting the changes of local

interactions as well as long-range interaction paths, e.g. indirect interactions between residues. It can be observed that most of the interactions present in the crystal structure are well represented in the simulated structure as well(gray nodes), however, the latter structure exhibits a significantly higher number of unique protein-protein interactions (red nodes) than the former(green nodes). This clearly indicates that a significant number of interactions are missed when ABCA1 structure is observed without a membrane emphasizing the need for studying membrane proteins in their lipid environment.

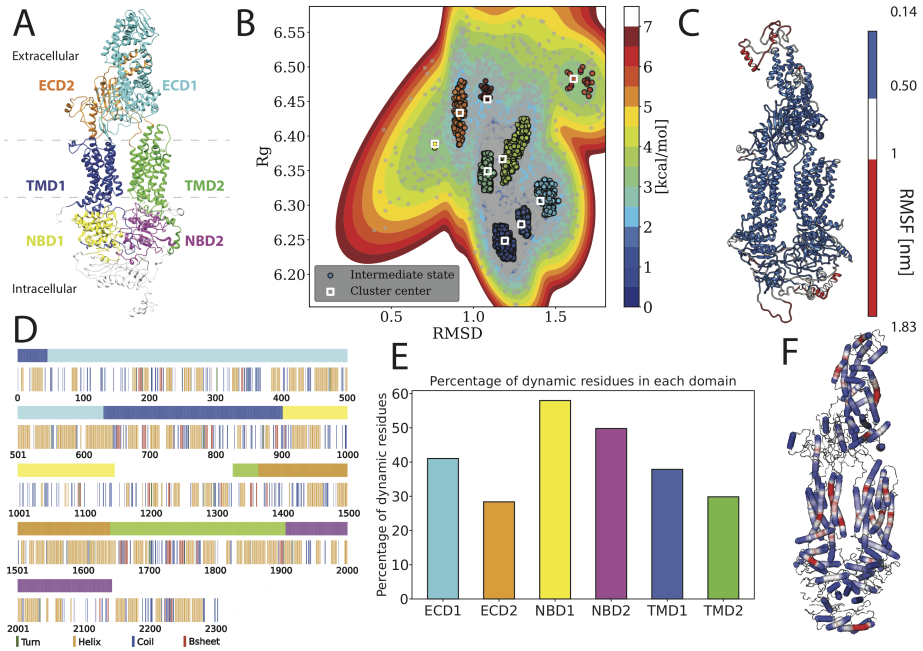

Figure 1: Protein-specific analysis. A. Domain assignment of ABCA1 according to Qian et al. B. Free energy estimation and clustering using InfleCS showed distinct minima bins C. Root mean square fluctuation (RMSF) mapped onto the protein reveals extremities of the protein being susceptible to large fluctuations. D. Residue-wise and domain-wise assignment of favoured secondary structure as well dynamic regions were identified where each domain is according to the 1A colour scheme (top bar) and the secondary structures are represented by green (turn), orange (helix), blue (coil) and red (beta-sheets) bars while the dynamic regions were left as white. E. Domain-wise percentage of dynamic residues , where the color of each bar corresponds to the domains in Panel A. F. Helical residues' degree of flexibility depicted by Red, indicating the areas of highest helix axis angle (>15°), followed by white for intermediate angle magnitudes (∼0-15°) and blue for angles close to, or at 0°.

Unraveling the influence of ABCA1 on membrane lipid dynamics. In order to understand the fate of lipids in the heterogeneous membrane due to presence of ABCA1, we calculated the average membrane thickness of both the outer as well as inner leaflet. The membrane thickness was observed to be fairly constant throughout all the five simulations (Figure 3A). The average thickness

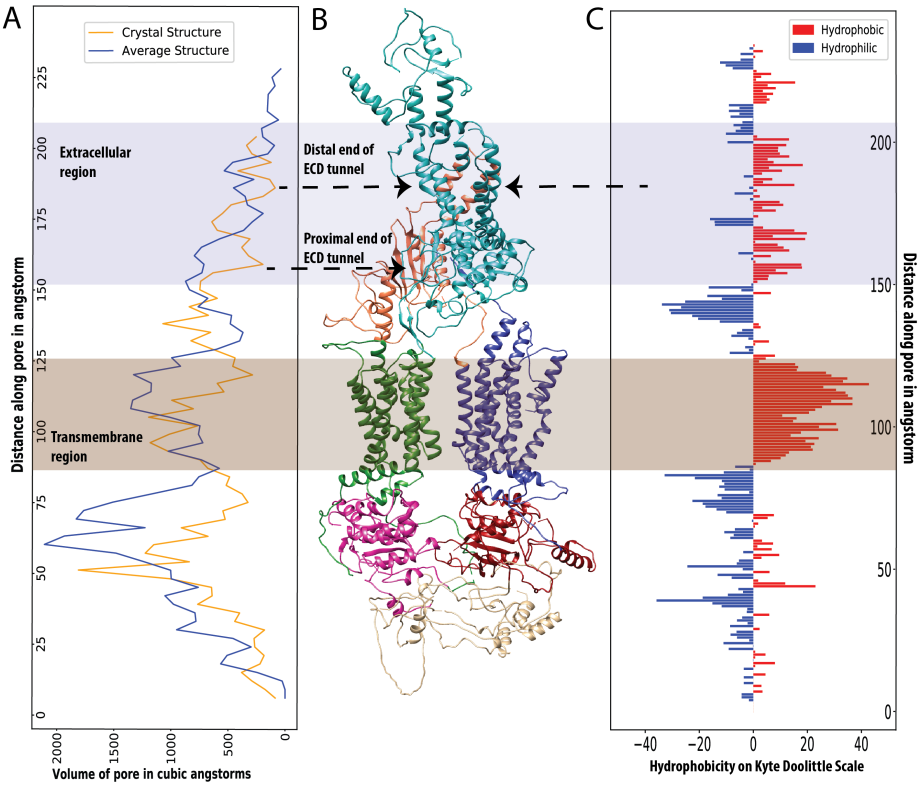

Figure 2: Functional characterization of the pore enclosed within ABCA1. A.Comparison of the volume profile of the pore enclosed within the crystal as well as simulation- stabilized structure. B. The distal as well as proximal ends of the tunnel enclosed within ECD1 (blue) and ECD2 (coral) have been highlighted. C. The hydrophobicity profile along the length of the pore (right).

of the bilayer ranged from 41.2 - 41.9 nm. Figure 3B depicts the time averaged deformation map for the top as well as the bottom leaflet. We observed that the outer leaflet experienced a positive deformation at the center while the lower leaflet underwent a negative deformation. These striking differences in membrane thickness implied that the presence of ABCA1 led the outer leaflet to be expanded while the lower leaflet appeared to be condensed at the site of implantation of protein in the bilayer. This is indicative of formation of a concave trough such that the membrane is found to curve at the center where the TMDs of ABCA1 are rooted. To ascertain whether any distortion was present in the membrane, mean curvature of both the leaflets were calculated. We observed that both the leaflets were found to be curved towards the middle of the bilayer at the points where the TMDs intersected with the bilayer (Figure 3C). This indicates that the presence of protein induces a curvature in the bilayer, compressing the bilayer, and thus potentially facilitating the transport of cholesterol. Intermolecular interactions at the bilayer interface owing two lipid tilt angles are known to affect the overall membrane organization as well as influence the helical tilt of the embedded region[22, 23]. Therefore, we utilized MEMBPLUGIN[24] to compute the lipid tilt angles of each of the lipid headgroups for each simulation. We observed that tilt angles for CHL1 ranged from 0 to 75°, while the rest of the lipids had similar tilts that ranged between 100 to 185° (Figure 3D). Interestingly, cholesterol tilt has been shown to influence bilayer organization. Cholesterol orientation perpendicular to the normal of bilayer is representative of an ordered bilayer, while changes in average cholesterol orientation were found to be strongly anti-correlated with membrane thickness[25]. Our results hint towards a similar phenomenon where presence of protein in the membrane influences the cholesterol tilt possibly resulting in the observed changes in membrane thickness causing it to expand or condense respectively (Figure 3B & C). Next, we wanted to understand the lipid dynamics that were at play. We performed clustering of each lipid type to generate separate heatmaps based on lipid counts around the protein. Supplementary Figure 7 depicts the spatial location of each of the lipid types around the protein. We observed that the most abundant lipid around the protein residues in both the top and bottom leaflet was POPC followed by PSM. Figure 3E illustrates the heatmap of PSM while Figure 3F represents the heatmap of POPC so obtained where the gradient colours represent lipid PSM or POPC molecules in the cluster while the blue squares represent the protein residues. While both the lipids did not appear to cluster as such, both POPC and PSM appeared to form a shell around the protein residues that were immersed in the membrane. Additionally, we also computed the average area spanned the heterogeneous membrane as a measure of its stability throughout our simulation (Supplementary Figure 8).

Understanding the protein-lipid interactions. Next we zoomed in on the protein residues that were found to interact with the surrounding membrane lipids for more than 500 ns throughout the simulation. We found around 156 such residues and the total number of interactions for each of these residues was quantified (Figure 4A). It can be seen that some of these residues (located at

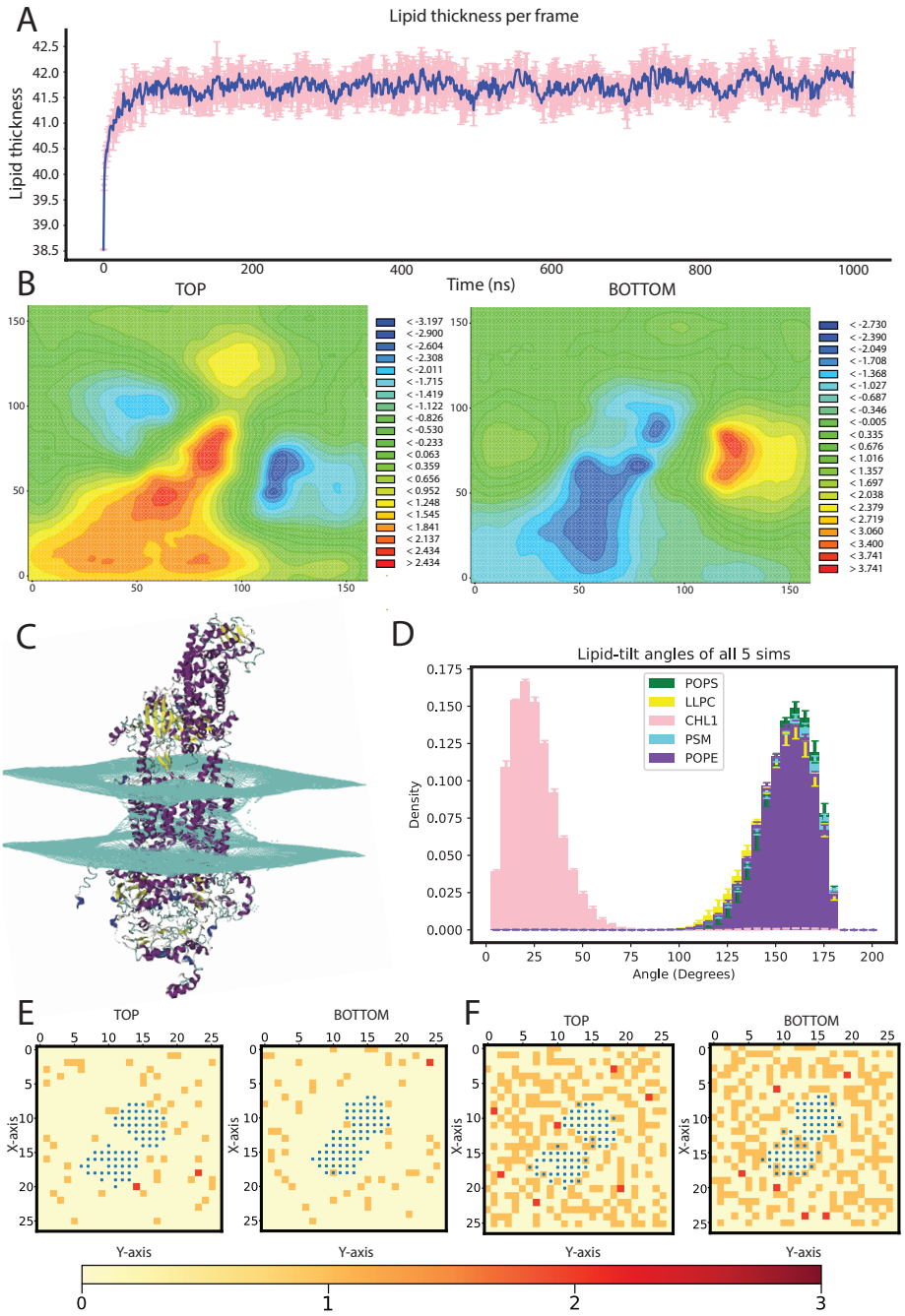

Figure 3: Lipid-specific analysis. A. Average membrane thickness throughout the simulation B. Heat maps depicting membrane thickness of the Top and Bottom leaflet of the membrane respectively. C. Membrane curvature induced due to protein D. Lipid-wise tilt distribution. Lipid clustering maps for E. PSM and F. POPC

the bottom of the heatmap) did not interact with any lipid residues initially (depicted in dark blue), but were found to form transient interactions with 1-4 lipid as the course of simulation progressed. All such protein-lipid interactions have been aggregated and depicted according to lipid types that they interact with in Supplementary Figure 9. Subsequently, we determined the different lipid types that surround the protein within a radius of 0.5nm throughout the simulation (Figure 4B). We assumed that these lipid residues may be interacting with the corresponding protein residues owing to their close vicinity. These results are in accordance with the lipid clustering analysis (Figure 3 E & F) showing that the most prevalent lipid type surrounding the protein is POPC followed by PSM. Next we analyzed, if any of the 156 residues that were found to actively interact with lipids throughout our simulation were implicated in any of the ABCA1 related disorders to extrapolate the importance of their interactions with surrounding lipids in protein stability or function. Residues amongst these 156 that were reported to be pathogenic or disease-related in either UniProt or dbSNP or both were assessed. Furthermore, SNPs&Go[26] was also used to ascertain the disease-association of the shortlisted nsSNPs. SNPs&Go results include, in addition to itself, predictions from PhD-SNP[27] and PANTHER[28]. 5 of the 156 residues (L715del, T795P, K797N, V846I, S1752C) were identified to have high probability to be disease causing. These were associated with pathogenic phenotype such as increased cardiovascular risk & increased plasma cholesterol levels. Figure 4D depicts the intensity of protein-protein contacts of these 5 residues while Figure 4E enumerates the number of protein-protein as well as protein-lipid interactions that these 5 residues participated in. Additionally it can be seen that these residues cluster mostly in TMD1 where it makes contact with the outer as well as inner leaflet. They were also found to interact with POPC and PSM mostly. Our results indicate that these residues are involved in several stabilizing protein-protein as well as protein-lipid interactions and therefore, mutations in these regions may be destabilizing in nature and/or affect protein function.

Conclusion. In this work we conducted all atom molecular dynamics simulation of monomeric ABCA1 in an explicit heterogeneous bilayer in order to elucidate the protein-membrane interactions that stabilize this ATP unbound form. We found that while the overall architecture of the protein from the crystal structure (5xjy) is maintained, there is a drastic increase in the volume of the central tunnel enclosed within the TMDs that leads upto the ECDs once the protein is immersed in a bilayer. Our structure also revealed that the tunnel enclosed within the ECDs that had previously been shown to taper at its distal end was wide enough to accommodate lipids. We believe that this tunnel within the ECDs could in fact serve as a reservoir for lipids. And once the lid of the ECD tunel moves away, facilitate an association with ApoA1 at the distal end to generate nascent HDL particles.

Additionally, we also observed that the presence of protein in the bilayer caused both the leaflets to fold inwards resulting in the formation of a concave trough where the protein intersects with the membrane. On analyzing the lipid

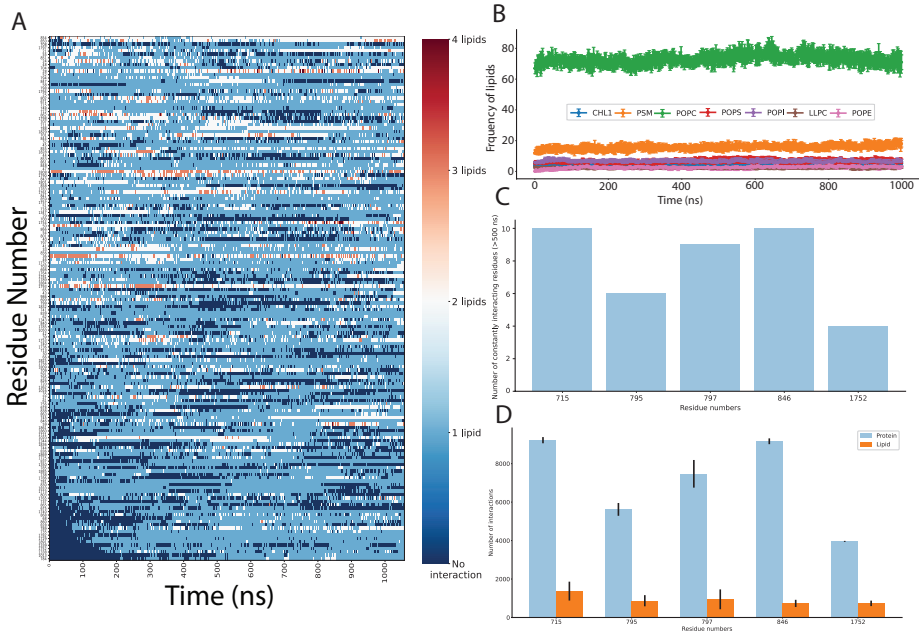

Figure 4: Protein-lipid interactions' analysis. A. Unique interactions of protein residues which interact with lipid residues for more than 500 ns B. Frequency of each lipid type surrounding the protein residues within a radius of 0.5nm throughout our simulation C. Number of protein-protein contacts made by the five disease-related protein residues D. Frequency of protein-protein and protein-lipid interactions of the five disease-related protein residues

dynamics we observed that POPC and PSM selectively formed a shell around the protein residues that are in contact with the membrane. These lipids had similar tilt angles while those of CHL1 were found to lie between 0-75° possibly leading to the observed changes in membrane thickness that may impact membrane order. We also quantified the number of interactions this structure makes with the bilayer and itself to ascertain residues in the TMD region that may be functionally important. Our analysis suggests that residues Leu 715, Thr 795, Lys 797, Val 846 and Ser 1752 make stabilizing interactions within the protein as well as with the membrane lipids and therefore providing a possible explanation for the high propensity of pathogenicity of nsSNPs in these regions.

In summary, we have attempted to refine the crystal structure of ABCA1 by embedding it in a heterogenous membrane and simulating it. Our observations highlight the need for studying membrane proteins in their lipid membrane environment allowing for resolution of the effect of membrane on protein and vice versa. We believe that this structure will aid in future work by allowing mechano-functional characterization of the protein at the membrane interface.

Acknowledgement. The authors would like to thank the HPC facility of IIIT Delhi for the computational facility.

Funding. S.S was supported by the CSIR-DBT funding agency. The study was supported by the Initiation Research Grant by IIIT Delhi for A.R.

The authors declare no competing interests..

References

[1] M. C. Phillips, Is abca1 a lipid transfer protein?, Journal of lipid research 59 (5) (2018) 749–763.

[2] A. Ji, J. M. Wroblewski, L. Cai, M. C. de Beer, N. R. Webb, D. R. van der Westhuyzen, Nascent hdl formation in hepatocytes and role of abca1, abcg1, and sr-bi, Journal of lipid research 53 (3) (2012) 446–455.

[3] R. M. Islam, M. Pourmousa, D. Sviridov, S. M. Gordon, E. B. Neufeld, L. A. Freeman, B. S. Perrin, R. W. Pastor, A. T. Remaley, Structural properties of apolipoprotein ai mimetic peptides that promote abca1-dependent cholesterol efflux, Scientific reports 8 (1) (2018) 1–15.

[4] R. J. Aiello, D. Brees, P.-A. Bourassa, L. Royer, S. Lindsey, T. Coskran, M. Haghpassand, O. L. Francone, Increased atherosclerosis in hyperlipidemic mice with inactivation of abca1 in macrophages, Arteriosclerosis, thrombosis, and vascular biology 22 (4) (2002) 630–637.

[5] E. Orsó, C. Broccardo, W. E. Kaminski, A. Böttcher, G. Liebisch, W. Drobnik, A. Götz, O. Chambenoit, W. Diederich, T. Langmann, et al., Transport of lipids from golgi to plasma membrane is defective in tangier disease patients and abc1-deficient mice, Nature genetics 24 (2) (2000) 192–196.

[6] H. Qian, X. Zhao, P. Cao, J. Lei, N. Yan, X. Gong, Structure of the human lipid exporter abca1, Cell 169 (7) (2017) 1228–1239.

[7] M. Hozoji, Y. Kimura, N. Kioka, K. Ueda, Formation of two intramolecular disulfide bonds is necessary for apoa-i-dependent cholesterol efflux mediated by abca1, Journal of Biological Chemistry 284 (17) (2009) 11293–11300.

[8] M. Ishigami, F. Ogasawara, K. Nagao, H. Hashimoto, Y. Kimura, N. Kioka, K. Ueda, Temporary sequestration of cholesterol and phosphatidylcholine within extracellular domains of abca1 during nascent hdl generation, Scientific reports 8 (1) (2018) 1–10.

[9] K. Nagao, K. Takahashi, Y. Azuma, M. Takada, Y. Kimura, M. Matsuo, N. Kioka, K. Ueda, Atp hydrolysis-dependent conformational changes in the extracellular domain of abca1 are associated with apoa-i binding, Journal of lipid research 53 (1) (2012) 126–136.

[10] Y. D. Landry, M. Denis, S. Nandi, S. Bell, A. M. Vaughan, X. Zha, Atp-binding cassette transporter a1 expression disrupts raft membrane microdomains through its atpase-related functions, Journal of Biological Chemistry 281 (47) (2006) 36091–36101.

[11] A. Zarubica, A. P. Plazzo, M. Stöckl, T. Trombik, Y. Hamon, P. Müller, T. Pomorski, A. Herrmann, G. Chimini, Functional implications of the influence of abca1 on lipid microenvironment at the plasma membrane: a biophysical study, The FASEB Journal 23 (6) (2009) 1775–1785.

[12] Y. Okamoto, M. Tomioka, F. Ogasawara, K. Nagaiwa, Y. Kimura, N. Kioka, K. Ueda, C-terminal of abca1 separately regulates cholesterol floppase activity and cholesterol efflux activity, Bioscience, biotechnology, and biochemistry 84 (4) (2020) 764–773.

[13] A. S. Oliveira, A. M. Baptista, C. M. Soares, Conformational changes induced by atp-hydrolysis in an abc transporter: A molecular dynamics study of the sav1866 exporter, Proteins: Structure, Function, and Bioinformatics 79 (6) (2011) 1977–1990.

[14] M. Miller, J. Rhyne, S. Hamlette, J. Birnbaum, A. Rodriguez, Genetics of hdl regulation in humans, Current opinion in lipidology 14 (3) (2003) 273–279.

[15] Y. Li, K. Tang, K. Zhou, Z. Wei, Z. Zeng, L. He, C. Wan, Quantitative assessment of the effect of abca1 r219k polymorphism on the risk of coronary heart disease, Molecular biology reports 39 (2) (2012) 1809–1813.

[16] A. R. Tanaka, S. Abe-Dohmae, T. Ohnishi, R. Aoki, G. Morinaga, K.-i. Okuhira, Y. Ikeda, F. Kano, M. Matsuo, N. Kioka, et al., Effects of mutations of abca1 in the first extracellular domain on subcellular trafficking and atp binding/hydrolysis, Journal of Biological Chemistry 278 (10) (2003) 8815–8819.

[17] K. Nagao, M. Tomioka, K. Ueda, Function and regulation of abca1–membrane meso-domain organization and reorganization, The FEBS journal 278 (18) (2011) 3190–3203.

[18] F. R. Marín-Martín, C. Soler-Rivas, R. Martín-Hernández, A. Rodriguez-Casado, A comprehensive in silico analysis of the functional and structural impact of nonsynonymous snps in the abca1 transporter gene, Cholesterol 2014 (2014).

[19] A. Zarubica, G. Chimini, Abca1, tangier disease, and lipid flopping, Transmembrane Dynamics of Lipids 9 (2011) 353.

[20] R. J. Suetani, B. Sorrenson, J. D. Tyndall, M. J. Williams, S. P. McCormick, Homology modeling and functional testing of an abca1 mutation causing tangier disease, Atherosclerosis 218 (2) (2011) 404–410.

[21] S. H. Hong, J. Rhyne, K. Zeller, M. Miller, Novel abca1 compound variant associated with hdl cholesterol deficiency, Biochimica et Biophysica Acta (BBA)-Molecular Basis of Disease 1587 (1) (2002) 60–64.

[22] K. Baczynski, M. Markiewicz, M. Pasenkiewicz-Gierula, Is the tilt of the lipid head group correlated with the number of intermolecular interactions at the bilayer interface?, FEBS letters 592 (9) (2018) 1507–1515.

[23] J. Le Coutre, L. Narasimhan, C. K. N. Patel, H. R. Kaback, The lipid bilayer determines helical tilt angle and function in lactose permease of escherichia coli, Proceedings of the National Academy of Sciences 94 (19) (1997) 10167–10171.

[24] R. Guixà-González, I. Rodriguez-Espigares, J. M. Ramírez-Anguita, P. Carrió-Gaspar, H. Martinez-Seara, T. Giorgino, J. Selent, Membplugin: studying membrane complexity in vmd, Bioinformatics 30 (10) (2014) 1478–1480.

[25] G. Khelashvili, G. Pabst, D. Harries, Cholesterol orientation and tilt modulus in dmpc bilayers, The Journal of Physical Chemistry B 114 (22) (2010) 7524–7534.

[26] E. Capriotti, R. Calabrese, P. Fariselli, P. L. Martelli, R. B. Altman, R. Casadio, Ws-snps&go: a web server for predicting the deleterious effect of human protein variants using functional annotation, BMC genomics 14 (3) (2013) 1–7.

[27] E. Capriotti, P. Fariselli, Phd-snpg: a webserver and lightweight tool for scoring single nucleotide variants, Nucleic acids research 45 (W1) (2017) W247–W252.

[28] H. Tang, P. D. Thomas, Panther-psep: predicting disease-causing genetic variants using position-specific evolutionary preservation, Bioinformatics 32 (14) (2016) 2230–2232.